CrossMark

ORIGINAL ARTICLE

Three-dimensional volume rendering of pelvic models and paraurethral masses based on MRI cross-sectional images

Stergios K. Doumouchtsis[1,2,3] · Daron A. Nazarian[2] · Nivedita Gauthaman[4] ·
Constantin M. Durnea[1] · Graham Munneke[5]

Abstract

Aims Our aim was to assess the feasibility of rendering 3D pelvic models using magnetic resonance imaging (MRI) scans of patients with vaginal, urethral and paraurethral lesions and obtain additional information previously unavailable through 2D imaging modalities.

Methods A purposive sample of five female patients 26-40 years old undergoing investigations for vaginal or paraurethral mass was obtained in a tertiary teaching hospital. 3D volume renderings of the bladder, urethra and paraurethral masses were constructed using 3D-Slicer v.3.4.0. Spatial dimensions were determined and compared with findings from clinical, MRI, surgical and histopathological reports.

The quality of information regarding size and location of paraurethral masses obtained from 3D models was compared with information from cross-sectional MRI and review of clinical, surgical and histopathological findings.

Results The analysis of rendered 3D models yielded detailed anatomical dimensions and provided information that was in agreement and in higher detail than information based on clinical examination, cross-sectional 2D MRI analysis and histopathological reports. High-quality pelvic 3D models were rendered with the characteristics and resolution to allow identification and detailed viewing of the spatial relationship between anatomical structures.

Conclusions To our knowledge, this is the first preliminary study to evaluate the role of MRI-based 3D pelvic models for investigating paraurethral masses. This is a feasible technique and may prove a useful addition to conventional 2D MRI. Further prospective studies are required to evaluate this modality for investigating such lesions and planning appropriate management.

Keywords Pelvic segmentation · 3D pelvic model · 3D volume rendering · Magnetic resonance imaging (MRI) · Urethral masses · Urethral diverticulum pelvic imaging

✉ Stergios K. Doumouchtsis
  sdoum@yahoo.com

1 Department of Obstetrics & Gynaecology, Epsom and St. Helier University Hospital NHS Trust, Epsom, UK

2 St George's University of London, London, UK

3 University of Athens, Athens, Greece

4 Department of Obstetrics &Gynaecology, Hampshire Hospitals NHS Foundation Trust, Hampshire, UK

5 St George's University Hospitals NHS Foundation Trust, London, UK

Introduction

Clinical diagnosis of paraurethral masses in women can be challenging, as most patients are asymptomatic [1, 2]. Typical presentation involves symptoms such as dysuria (30–70%), postmicturition dribbling (10–30%) and dyspareunia (10–25%), commonly named the three Ds [3, 4]. The anatomical location of the urethra lends itself to being vulnerable to infection or trauma. Mainly found in the mid or distal urethra, common lesions such as urethral diverticula are increasing in incidence primarily due to improved diagnostic clinical and imaging capabilities [5].

Imaging techniques play a vital role both in the diagnostic process and preinterventional evaluation of paraurethral masses. When symptomatology is nonspecific and only 50–60% of diverticula are diagnosed by physical examination, further investigation becomes necessary [1] for accurate diagnosis. Magnetic resonance imaging (MRI) is a noninvasive modality effective in visualising paraurethral masses when

compared with other techniques. Considering the greater anatomical detail rendered through higher resolution, multidirectional imaging and greater tissue contrast, MRI plays an important and reliable diagnostic, investigative and presurgical planning role for gynaecological and obstetric pathology [4, 6–8]. Diagnosis and classification of pathology has traditionally been achieved using 2D cross-sectional imaging; however, 3D imaging appears superior for identifying complex anatomical areas such as the female pelvis [9, 10].

Additionally, the presumed clinical applicability and anatomical integrity of a 3D model may improve our diagnostic skills and interventional planning. Three-dimensional models play an important role in neurosurgery, vascular, hepatic and orthopaedic surgery [10–16]. Pelvic surgeons, however, remain primarily reliant on the interpretation of 2D cross-sectional imaging [11]. We attempted to render 3D models of paraurethral structures and pathology of the pelvis in female patients using conventional 2D MRI images. The primary aim of this study was to evaluate the feasibility of rendering 3D models in these patients and to obtain additional quantitative information unavailable through conventional 2D investigative modalities.

Materials and methods

Copies of anonymised MRI scans of the pelvis were obtained from the Radiology Department. We selected scans of five women aged between 26 and 40 years of age undergoing investigations for a suspected vaginal/paraurethral mass over a year's period. We selected cases representing a range of such lesions in order to evaluate the ability of the technique to be applied in different clinical scenarios. Inversion recovery (IR) and T1- and T2-weighted spin-echo images were obtained from a 1.5-Tesla magnet (Signa HDxt, GE Medical Systems, Milwaukee WI, USA). Patients were positioned feet first supine, and MRI sequences included IR, T1- and T2-weighted axial, coronal and sagittal images; high-resolution T2-weighted coronal and axial, and T1 fat-saturated axial fast spin-echo sequences across the five patients. Each series contained ~20 images, with slice thicknesses of 3-5mm and spacing between slices of 4-5.5 mm. Resultant data were provided in Digital Imaging and Communication in Medicine (DICOM) format. An open-source software package, 3D Slicer v.3.4.0 (Brigham and Women's Hospital, Harvard Medical School, Boston, MA, USA), was used for image analysis, visualisation, segmentation, label mapping and 3D volume rendering (Fig. 1).

Patient demographic data including age and parity, relevant past medical and surgical history, clinical and surgical findings, data from MRI reporting and histopathological reporting of the lesions were obtained from the NHS Electronic Patient Records (EPR). and demographic data from the EPR patient profile. These results were anonymised and transferred onto a Microsoft Excel® (2010) spreadsheet for analysis and comparison with 3D modelling analysis findings (Table 1).

This study was approved as an audit by our institutional Audit Department (Audit No 333).

Identifying cross-sectional anatomy across all three visual planes

First, the midsagittal plane was identified from the MRI series to study the appropriate cross-sectional anatomy and specifically structures identifiable on all three planes. Once these structures and anatomical relationships were established, the appropriate slices in both axial and coronal planes were determined, identifying their number, size, shape and relationship to surrounding structures. Corresponding views of the highlighted structure in one plane were simultaneously revealed in the other two visual plane slices, enabling the marrying of individual voxels (a unit of graphic information that represents a point in a 3D space) seen on an image in one orthogonal plane with the corresponding view in the other two planes. The segmentation of anatomical structures and creation of image subsets by partitioning specific sections of an original image corresponding to the desired structures is a vital first step in the creation of a 3D visualisation. From these segmented structures, a label map—a 3D scalar volume in which each voxel within that volume is allocated a colour indicating tissue type at that location—was then created. The three-number label map was generated with each number corresponding to the appropriate tissue type and a colour designated to that number by the programme. Of the three image series—sagittal, coronal and axial—each series contained three label maps: 1× bladder, 1× urethra and 1× lesion(s) individually colour coded. From a single image series, a merge volume (temporary copy upon which label maps were then created) was generated. Upon completion of all three label maps (one for each of the three targeted anatomical structures), the merge volume was superimposed onto the master volume (original image series), with the bladder highlighted in pink, urethra in light blue and lesion in yellow. Each patient data set would therefore contain three merge volumes (each corresponding to a single visual plane), with each merge volume containing three label maps (each corresponding to a single targeted anatomical structure). This process was repeated for the remaining series representing the two remaining visual planes, resulting in nine label maps per patient (three planar views with three structures highlighted in each), thus optimising anatomical accuracy of the resultant model.

Volume rendering: creating a 3D model

Once all nine label maps for a single patient were created, the 3D model was generated. Initially, an image series representing one of the visual planes was selected containing its three label maps. A 3D surface model was rendered using
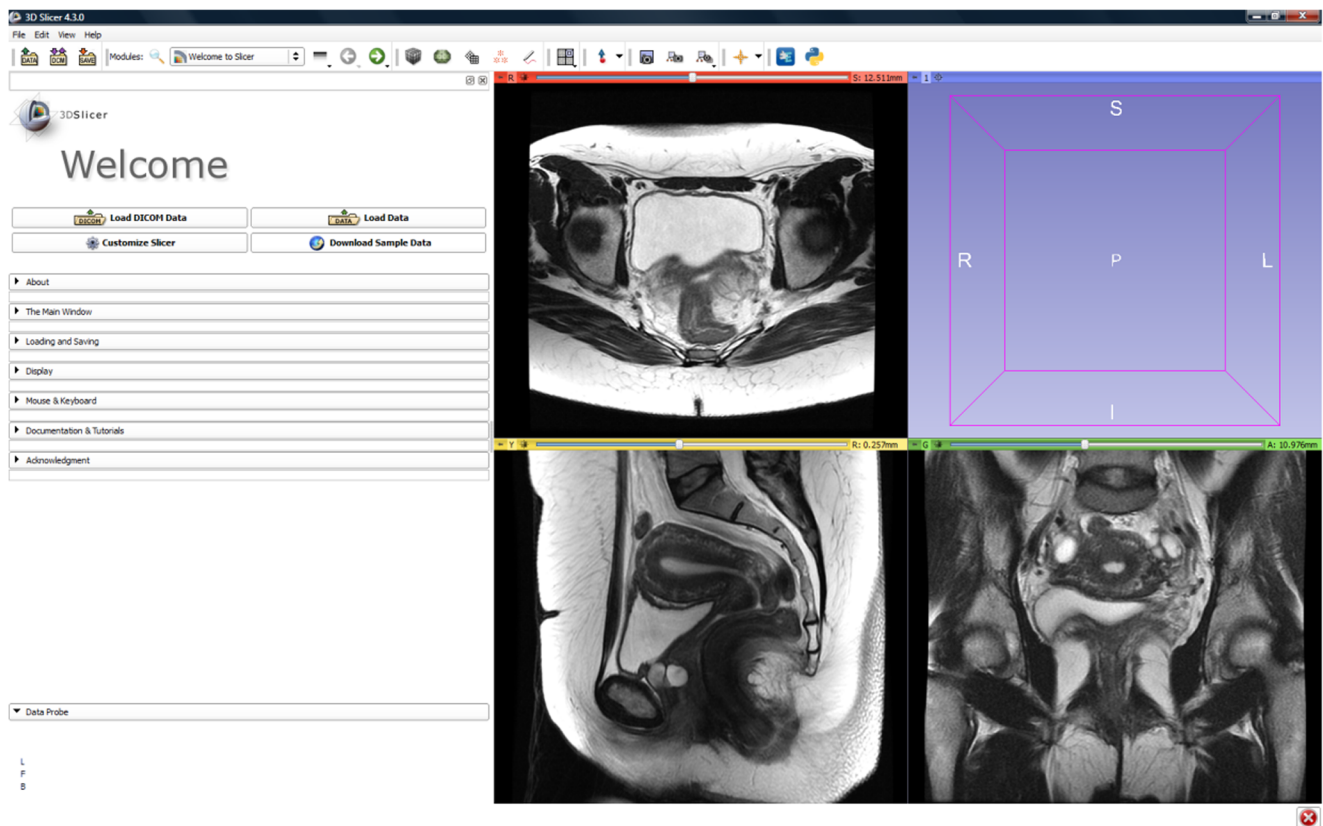
Fig. 1 Three-dimensional Slicer UI with axial (*red*), sagittal (*yellow*) and coronal (*green*) T2-weighted magnetic resonance image series of the pelvis from a single patient

Table 1 Clinical, magnetic resonance imaging (MRI), surgical and histopathological reporting for all five patients

	Demographics	Clinical presentation	Clinical diagnosis	MRI report	Surgical report	Histopathology
1	40 years, black, para 3	Mixed urinary incontinence, palpable suburethral mass	Urethral diverticulum 6 mm × 9 mm	Urethral defect at 5 o'clock, small collapsed diverticulum 6 × 9 mm	Urethral diverticulum 10 × 20 mm at 5 o'clock, 1 cm from external meatus	20 × 10 × 10-mm urethral diverticulum
2	40 years, white European, para 3	Recurrent stress urinary incontinence, suburethral mass	Grade 2 urethrocele, ? suburethral cyst	3 septated cysts around proximal urethra, 14 × 13, 15 × 10 and 13 × 9 mm, likely bulking material	Not applicable	Not applicable
3	36 years white European, para 2	Stress urinary incontinence, vaginal mass	30-mm cyst in R anterior vaginal fornix	R lateral vaginal wall cyst 38 × 15 × 14 mm with septations	40-to 50-mm R anterolateral vaginal wall cyst	Not applicable
4	36 years, Chinese, para 2	Vaginal lump, minor stress urinary incontinence	Grade 1 cystocele, 2× paraurethral cysts: 1× R suburethral 5 × 10 mm 1× R lateral wall 5 × 10 mm	3× paraurethral cysts, no urethral connection, R 15 mm, 11 mm, L 12 mm	EUA: 2 paraurethral cysts, no connection to urethra, not excised	Not applicable
5	26 years, white European, para 1	Vaginal lump, Intermittently draining milky fluid via urethra	30 to 40 mm urethral diverticulum	Urethral diverticulum 8 × 23 mm	Urethral diverticulum 30–40 mm	25 × 20-mm urethral diverticulum

EUA examination under anaesthesia, *R* right, *L* left

data from the three label maps in that single series. This produced a model of the bladder, urethra and lesion(s) as seen from a single visual plane, with each structure coloured differently according to its tissue type (paraurethral mass is yellow-green) (Fig. 2). The model itself is a polyhedral structure composed of interlocking volumetric meshes, establishing a representation of both surface and volume of the highlighted anatomy. Inadequate surface models, resulting from incorrect structure demarcation, were revised following input from a consultant radiologist (GM) who reviewed all label maps prior to final rendering. Repeating this process for the image series of the remaining two visual planes created a consolidated final model rendering the bladder, urethra and lesion(s) in three dimensions (Fig. 3).

Linear measurements

With fiducial markers placed within the 3D model, 3D slicer used the x, y and z coordinate values to calculate the distance between fiducials and thus provided information pertaining to dimensions of and distances between the various anatomical landmarks under scrutiny. The distance between the proximal

aspect of the paraurethral pathology and the bladder neck as well as the distance between the distal aspect of the mass and the external urethral meatus was calculated using the same method. The measurements were then transferred onto a Microsoft Excel (2010) spreadsheet for further analysis (Table 2).

Results

Of the five women studied, two were diagnosed with urethral diverticula, one with a Gartner's cyst, one with paraurethral cysts and one with masses corresponding to previous bulking procedures for stress urinary incontinence. Four women presented with stress urinary incontinence and four with a palpable vaginal/paraurethral mass.

High-quality 3D volume renderings were created by the 3D Slicer programme (Fig. 4). Each slice contained enough detail to enable identification of pertinent anatomical structures and to identify relationships between them. An independent model was created in which the operator could zoom into specific locations for more detailed viewing of spatial anatomical relationships, rotate the model to view structures from differing planes
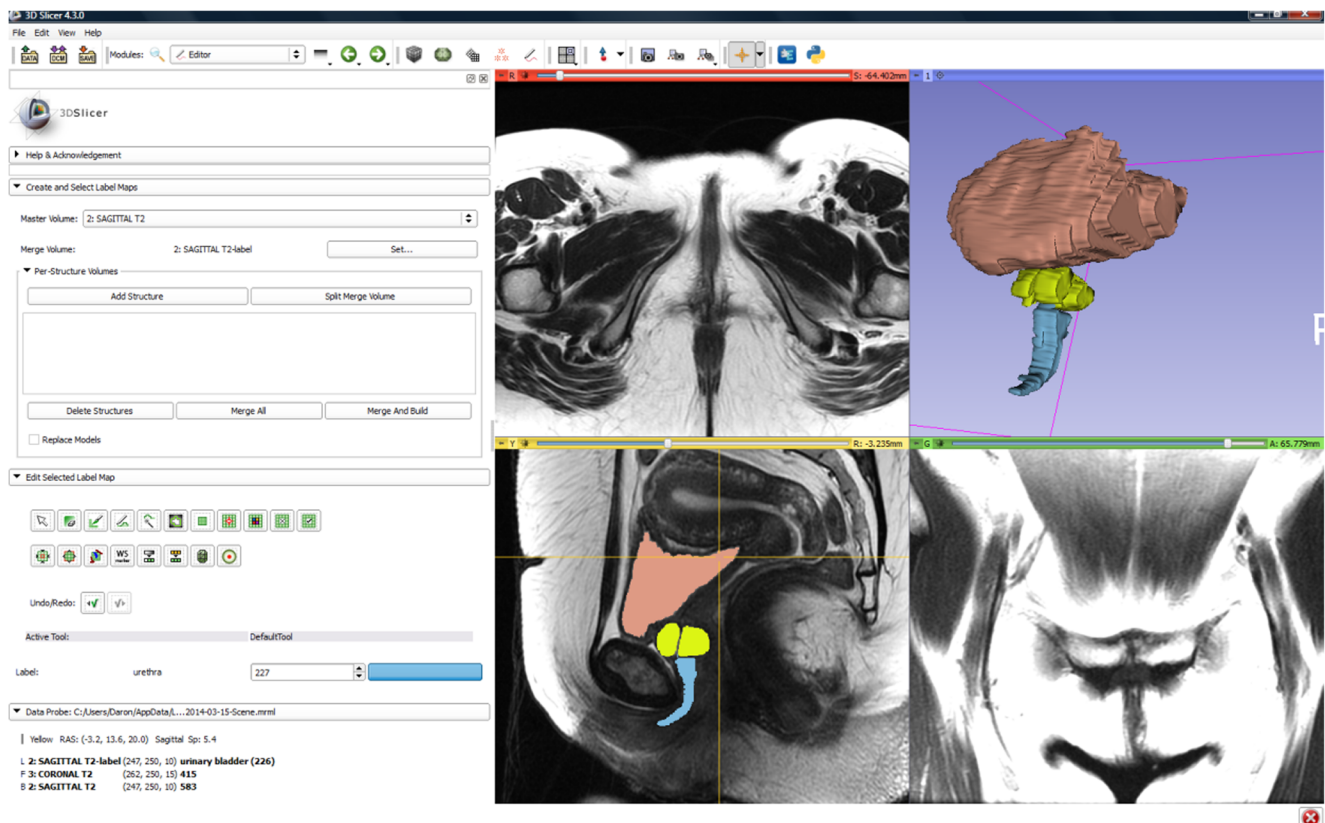

Fig. 2 Three-dimensional surface rendering of the bladder (*pink*), urethra (*blue*) and paraurethral mass (*yellow*) from sagittal label maps only. The upper right quadrant displays the rendered 3D surface model
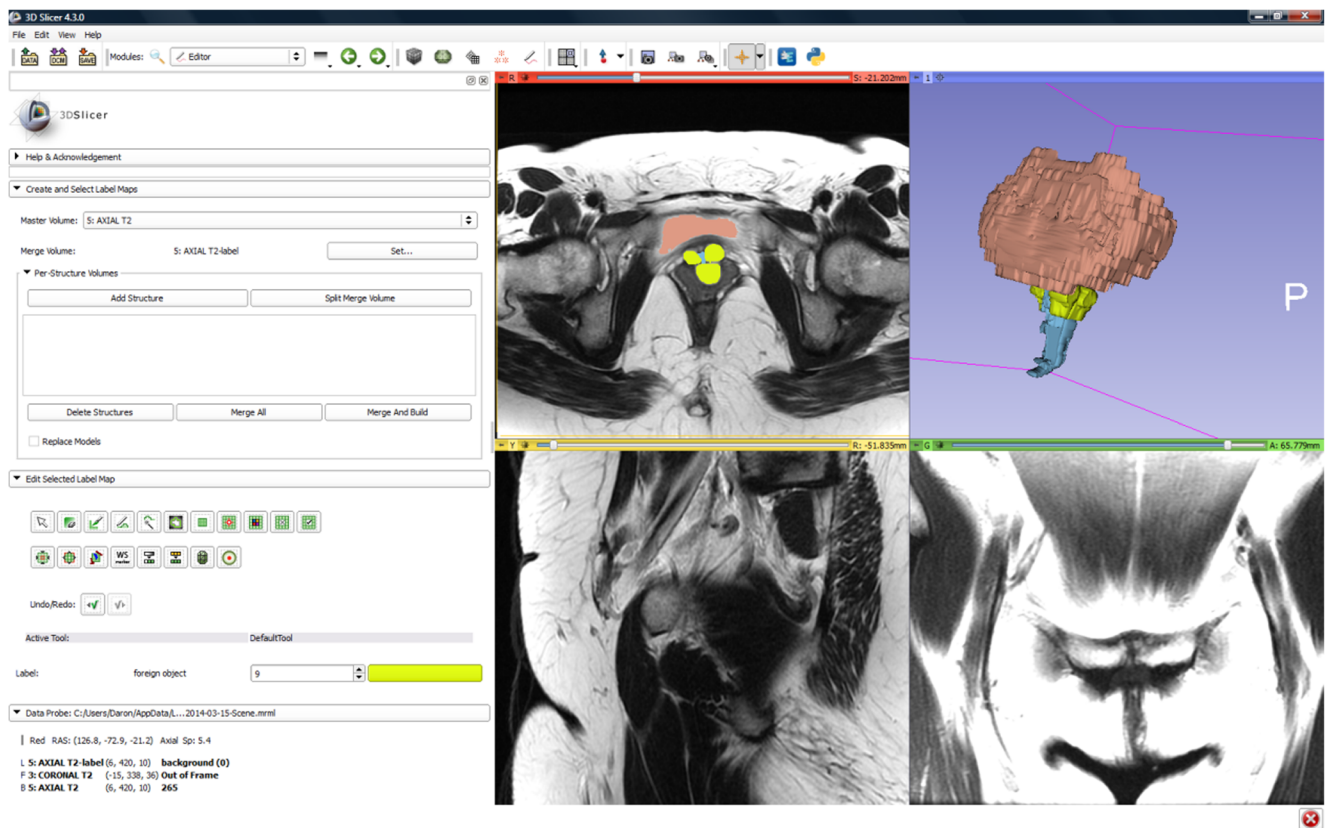
Fig. 3 Fully-rendered 3D model of the bladder (*pink*), urethra (*blue*) and paraurethral mass (*yellow*) combining data from axial, sagittal and coronal label maps prior to smoothing. The upper right quadrant displays the rendered 3D surface model

and hide and retrieve structures, allowing the anatomy of deeper structures to be visualised. The models had further applicability: using 3D Slicer, the models were superimposed onto the 2D slices of all three planes both individually and simultaneously. This enabled the simultaneous observation of the relationship between rendered 3D structures and the 2D anatomy (Fig. 5).

Mass dimensions as measured using the 3D Slicer provided data to 2 decimal places each time, and calculating the distance between masses and identifiable structures was possible. Specifically, it was possible to measure the distance between masses, urethral meatus and bladder neck. Bladder and urethra dimensions were measured.

Discussion

Main findings

Results confirm that 3D volume rendering of vaginal and paraurethral lesions based on MRI is a feasible technique with the potential to provide detailed anatomical information previously unavailable to clinicians relying on 2D imaging modalities alone. Linear dimensions of paraurethral/vaginal masses for all five patients were determined. Variations in reported dimensions of the masses under investigation or treatment are probably secondary to their cystic nature, with resultant temporal variations in fluid volumes. However, it was possible to estimate the distance of the masses from the urethral meatus and bladder neck using this technique.

Strengths and limitations

Can 3D volume rendering provide more accurate dimensional data of pelvic structures and pathology?

Without 3D measurements, the position, extent and relationship of the mass to adjacent anatomical structures is determined with less detail. Subsequently, the ability to perform clinical assessment and surgical planning based on anatomical relationships may be suboptimal. Measurements describing the spatial relationship of these pelvic structures cannot be obtained accurately using a conventional 2D imaging modality, since diagonal distances running between slices cannot be measured. When slice thickness ranges from 3 to 5 mm and the distance between slices is 4–5.5 mm, the margin of error for any potential method of extrapolating that distance is likely too large to be acceptable in a

Table 2 Data calculated from the analysis of 3D models showing craniocaudal height, longitudinal width and depth dimensions (mm) taken from two planes, with the mean calculated for bladder, urethra and lesions(s)

Structure	Height			Width			Depth			Distance from proximal aspect of lesion/mass to bladder neck	Distance from distal aspect of lesion/mass to external meatus
	Sagittal	Coronal	Mean	Coronal	Axial	Mean	Sagittal	Axial	Mean		
Patient 1											
Bladder	64.70	61.90	63.30	80.70	90.70	85.70	67.90	79.40	73.65	–	–
Urethra	38.30	34.10	36.20	13.10	19.10	16.10	15.40	17.10	16.25	–	–
Lesion/Mass	6.62	6.29	6.46	9.20	8.90	9.05	4.49	5.90	5.20	19.10	21.50
Patient 2											
Bladder	56.40	59.10	57.75	87.80	94.50	91.15	58.00	60.50	59.25	–	–
Urethra	61.40	54.90	58.15	13.60	14.20	13.90	8.17	14.50	11.34	–	–
Lesion/Mass left	16.40	17.10	16.75	11.60	10.60	11.10	10.80	10.20	10.50	5.23	33.90
Lesion/Mass right	13.70	15.00	14.35	8.78	8.62	8.70	7.56	8.87	8.22	9.38	33.00
Lesion/Mass rear	15.00	15.20	15.10	17.20	16.00	16.60	14.80	14.80	14.80	14.50	35.30
Patient 3											
Bladder	39.30	48.70	44.00	80.70	87.80	84.25	46.10	46.70	46.40	–	–
Urethra	33.20	34.90	34.05	14.00	13.40	13.70	11.80	14.20	13.00	–	–
Lesion/Mass	36.80	39.80	38.30	18.60	21.80	20.20	14.30	14.20	14.25	36.70	30.90
Patient 4											
Bladder	36.60	39.76	38.18	66.50	75.81	71.16	37.50	35.60	36.55	–	–
Urethra	36.70	33.60	35.15	16.40	15.20	15.80	12.26	15.10	13.68	–	–
Lesion/Mass left	15.41	13.90	14.66	7.43	8.69	8.06	12.41	11.50	11.96	21.40	21.60
Lesion/Mass right	13.90	14.02	13.96	9.26	9.42	9.34	10.38	13.10	11.74	20.90	22.10
Lesion/Mass inferior	11.20	11.31	11.26	9.94	10.10	10.02	8.05	11.20	9.63	24.20	18.00
Patient 5											
Bladder	13.25	12.10	12.68	64.60	32.80	48.70	59.01	27.60	43.31	–	–
Urethra	33.52	39.60	36.56	15.00	15.56	15.28	12.66	15.27	13.96	–	–
Lesion/Mass	20.91	21.27	21.09	10.91	11.30	11.11	8.36	8.36	8.36	18.70	5.12

Spatial relationship between lesion(s)/mass(es) and urethral landmarks (mm) are shown

clinical or presurgical setting. The most labour-intensive aspect of this study was the model rendering itself. The time required to complete this depends on the familiarity and experience of the operator with the software. Once this task was complete, further analysis yielding additional highly detailed information became possible to complete in a short time frame without the requirement of additional expertise. This allowed the relationship between proximal mass to bladder neck and distal mass to urethral meatus to be determined quickly enough for this data to be valuable in the clinical setting.

Further improvements to the technique of manual segmentation are required, since operator bias and the time-consuming examination of each 2D slice within a series are potential limiting factors. Furthermore, all volume-rendering processes generate noise artefacts during volume construction, rendering inaccurate regions or boundary discontinuities. In this study, postrendering Laplacian smoothing of the model with manual configuration of the smoothing iterations achieved optimum noise attenuation. The final limitation is that models were generated from MRI images with slice thicknesses between 3 and 5 mm. Future prospective MRI data sets with slices of 1-mm thick would maximise the accuracy of the resultant models.

Interpretation

Does 3D volume rendering have a place in augmenting presurgical planning?

The 3D models rendered provide a detailed view of relationships between anatomical structures within the female pelvis and thus have the potential to fulfil a role as a surgical guidance and visualisation system. Image- guided surgical systems augment the surgeon's capability of increasing accuracy and safety while decreasing invasiveness using medical imaging [17].

Fig. 4 Three-dimensional surface renderings of five patients with suspected paraurethral or paravaginal masses. Bladder (*pink*), urethra (*blue*), pathology (*yellow*). **a** Bulking-procedure-related masses, **b** urethral diverticulum, **c** Gartner's cyst, **d** paraurethral cysts ×3, **e** urethral diverticulum
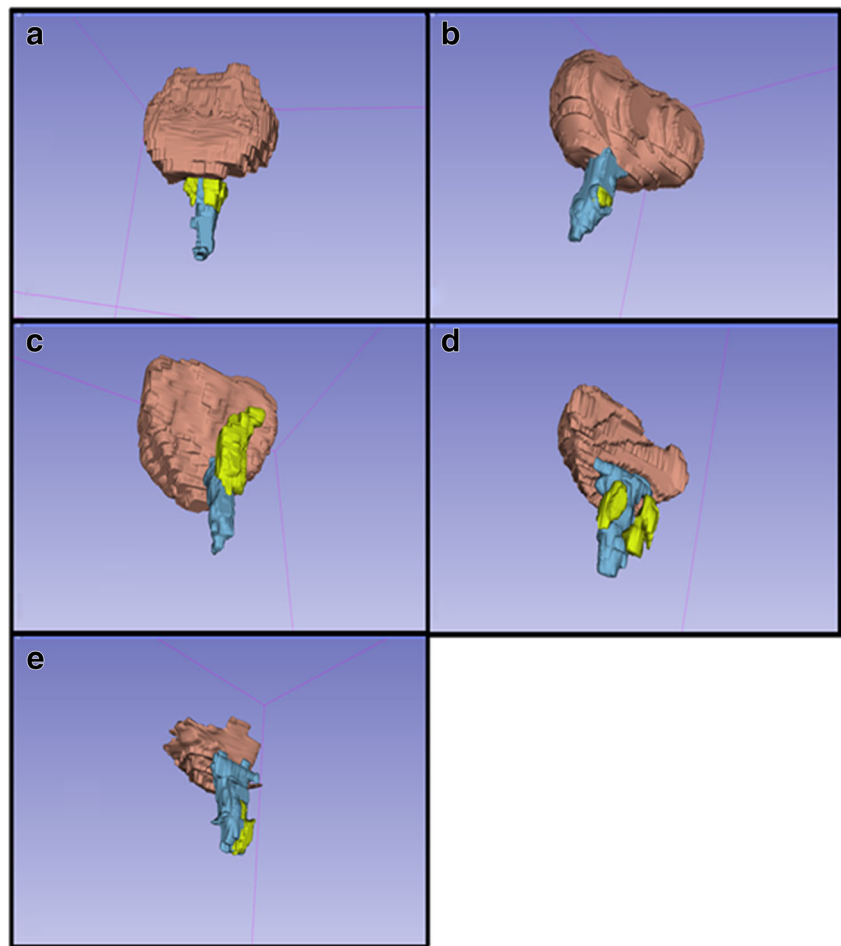
Is 3D modelling based on MRI superior to 3D or 4D ultrasound in volume rendering and image acquisition?

To answer this question, a comparative study between the two modalities is necessary. Nardos et al. [18] compared levator hiatus measurements between pelvic MRI and 3D pelvic ultrasound (US). They found that MRI measurements obtained from sagittal images were consistently greater than those obtained by US. However, there was no such difference between MRI and US for axial images. The authors attributed this observation to acquisition planes for axial images or interpretation of landmarks for sagittal images. This example highlights the importance of comparing like for like, i.e., volume-rendered models based on MRI and similar models based on US.

Conclusions

Paraurethral lesions, while comparatively rare, are commonly asymptomatic and are thus difficult to diagnose. Subsequently, the true prevalence is likely to be higher than currently reported. Two-dimensional cross-sectional imaging including MRI provides the most comprehensive evaluation and is considered both an initial investigation and a secondary modality for use when results from clinical investigation or alternative imaging remain inconclusive.

This study shows that 3D constructions of the female pelvic floor structure is technically feasible based on routine MRI. Greater detail is provided both for anatomical dimensions and relationships between paraurethral lesions and urethra and adjacent structures (such as bladder neck and urethral meatus) compared with conventional 2D imaging alone for clinical use. Greater detail can be achieved to ascertain anatomical dimensions of lesions by using 3D models rather than clinical analysis and 2D imaging alone. Furthermore, the model allows determining distances between anatomical structures, providing information that was unknown when these patients were initially investigated.

Analysis of 3D volumetric models may have a role in presurgical planning, with integration into intraoperative image-guided treatment being an exciting new front. Multiple data sets can be combined to form a 3D visualisation
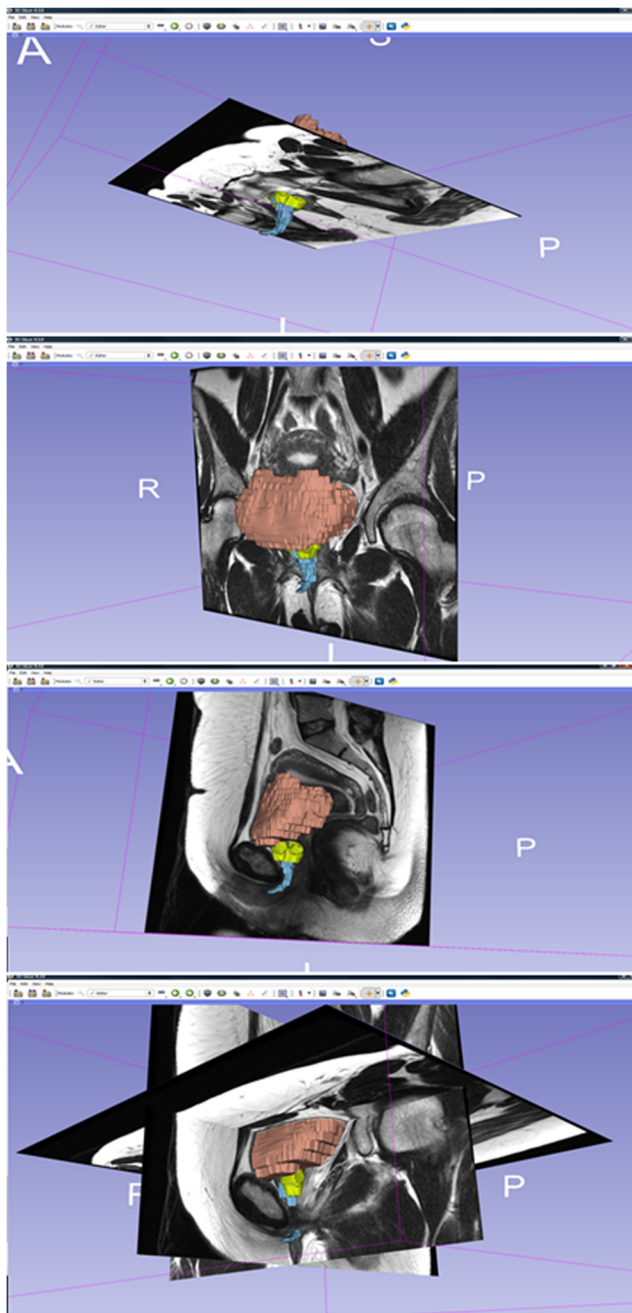
Fig. 5 Three-dimensional model superimposed onto 2D series: sagittal view (*top*), axial view (*upper middle*), coronal view (*lower middle*) and all three views simultaneously (*bottom*). Bladder (*pink*), urethra (*blue*), pathology (*yellow*)

accurate algorithms and their integration into existing software seems highly likely.

Further studies examining the impact of 3D volume rendering on medical education would herald the development of a potential new gold standard of anatomy instruction. This would allow students and instructors to interact and alter 3D models in real time, visualising the architecture of both anatomy and pathology in a patient to a degree of accuracy never before attained.

Compliance with ethical standards

Conflict of interest   None.

Funding   None.

References

1. Mangera A, Patel AK, Chapple CR. Anatomy of the lower urinary tract. Surg – Oxford Int Ed. 2010;28(7):307–13. doi:10.1016/j.mpsur.2010.03.002.
2. Patel AK, Chapple CR. Female urethral diverticula. Curr Opin Urol. 2006;16(4):248–54.
3. Bennett SJ. Urethral diverticula. Eur J Obstet Gynecol Reprod Biol. 2000;89(2):135–9.
4. Venyo AKG, Gopall A. Female urethral diverticula: a review of the literature. Webmed Central Urol. 2012;2012;3(5). doi:10.9754/journal.wmc.2012.003428.
5. Romanzi LJ, Groutz A, Blaivas JG. Urethral diverticulum in women: diverse presentations resulting in diagnostic delay and mismanagement. J Urol. 2000;164(2):428–33.
6. Lee JW, Fynes MM. Female urethral diverticula. Best Pract Res Clin Obstet Gynaecol. 2005;19(6):875–93.
7. Finch WJG, Webb RJ. Female urethral diverticula. Trends Urol, Gynaecol Sexual Health. 2008;13(4):22–3. doi:10.1002/tre.75.
8. Hricak H. MRI of the female pelvis: a review. AJR Am J Roentgenol. 1986;146(6):1115–22.
9. Müller-Stich BP, Löb N, Wald D, Bruckner T, Meinzer H, Kadmon M, et al. Regular three-dimensional presentations improve in the identification of surgical liver anatomy – a randomized study. BMC Med Educ. 2013;25(13):131–8.
10. Falchi M, Rollandi GA. CT of pelvic fractures. Eur J Radiol. 2004;50(1):96–105.
11. Kraima AC, Smit NN, Jansma D, Wallner C, Bleys RL, van de Velde CJH, et al. Toward a highly-detailed 3D pelvic model: approaching an ultra-specific level for surgical simulation and anatomical education. Clin Anat. 2013;26(3):333–8.
12. Beriault S, Al Subaie F, Mok K, Sadikot AF, Pike GB. Automatic trajectory planning of DBS neurosurgery form multimodal MRI datasets. Med Image Comput Comput Assist Interv. 2011;14:259–66.
13. Lesage D, Angelini ED, Bloch I, Funka-Lea G. A review of 3D vessel lumen segmentation techniques: models, features and extraction schemes. Med Image Anal. 2009;13(6):819–45.
14. Debarba HG, Zanchet DJ, Fracaro D, Maciel A, Kalil AN (2010). Efficient liver surgery planning in 3D based on functional segment classification and volumetric information. Conf Proc IEEE Eng Med Biol Soc, 4797-4800.

that can be quickly analysed, providing information supplementary to that gained by direct visualisation for application by the surgeon in real time. Consequently, developments in this field will include reliable and accurate automatic segmentation and volume-rendering techniques, making 3D model construction less labour intensive. Existing algorithms are not accurate enough to rely on; however the development of

15. Reitinger B, Bornik A, Beichel R, Schmalstieg D. Liver surgery planning using virtual reality. IEEE Comput Graph Appl. 2006;26(6):36–47.

16. Heng PA, Cheng CY, Wong TT, Wu W, Xu Y, Xie Y, et al. Virtual reality techniques. application to anatomic visualization and orthopaedics training. Clin Orthop Relat Res. 2006;442:5–12.

17. Jolesz FA, Nabavi A, Kikinis R. Integration of interventional MRI with computer-assisted surgery. J Magn Reson Imaging. 2001;13(1):69–77.

18. Nardos R, Thurmond A, Holland A, Gregory WT. Pelvic floor levator hiatus measurements: MRI versus ultrasound. Female Pelvic Med Reconstr Surg. 2014;20:216.